# CHARACTERIZATION OF INDOOR AND OUTDOOR POOL FIRES WITH ACTIVE CALORIMETRY*

**J. A. Koski, W. Gill, L. A. Gritzo, L. A. Kent**
Sandia National Laboratories
Albuquerque, New Mexico

**S. D. Wix**
Gram, Inc.
Albuquerque, NM

## ABSTRACT

A water cooled, 1 m x 1 m, vertical calorimeter panel has been used in conjunction with other fire diagnostics to characterize a 6 m x 6 m outdoor and three 3m x 3m indoor JP-4 pool fires. Measurements reported include calorimeter surface heat flux and surface temperatures, flame temperatures, and gas flow velocities in the fire. From the data, effective radiative absorption coefficients for various zones in the fires have been estimated. The outdoor test was conducted at Sandia's Coyote Canyon test facility, while indoor tests were conducted at the indoor SMokE Reduction Facility (SMERF) at the same location. The measurements provide data useful in calibrating simple analytic fire models intended for the analysis of packages containing hazardous materials.

## INTRODUCTION

Packages for shipment of radioactive materials are designed to withstand a 30 minute fully engulfing exposure to a large open pool fire. Presently, initial analyses of such shipping containers are usually done with a simple transparent medium radiative heat transfer model that ignores much of the physics that is known to affect heat fluxes in fires. For example, in contrast with the simple uniform surface heat flux models in use, testing has shown that local surface heat fluxes to packages vary depending on height above the pool, mass of the container, surface orientation and other variables [1,2]. Nicolette and Larson [3] examined these effects with a relatively simple participating medium radiative heat transfer model and were able to identify probable causes for many of the experimentally observed phenomena. The major thrust of the work described here is to provide an experimental basis that extends the simple participating medium models that have been developed into tools that can accurately predict the interaction between fires and the packages in the fire. Such a tool will increase confidence in package design, improve the likelihood that the package will successfully pass regulatory tests, and result in a safer package during actual accidents.

Most heat flux measurements made to date in large pool fires relied on transient temperature measurements of massive objects with data analysis through inverse heat conduction methods [1,2,4]. To complement this approach by fixing several fire variables, experiments with an actively cooled calorimeter in a large pool fire have been completed, and some results are reported here. By water cooling the fire-exposed face of the calorimeter, surface temperature variations with time and location are minimized, and quasi-steady-state heat fluxes can be determined from the temperature rise and flow rate of the cooling water. Segmentation of the face into zones also allows determination of the vertical absorbed heat flux profile. The emitted heat flux (i.e. the surface emissive power) was measured with intrinsic thermocouples installed on the actively-cooled calorimeter surface. Fire environment measurements were obtained using a velocity probe, and an array of sheathed thermocouples and Directional Flame Thermometers (DFTs) mounted in front of the calorimeter which provide a distribution of fire temperature and heat fluxes, respectively. The goal of the program is to gather experimental data that will be used to calibrate analytical fire submodels [3,5,6] that can be coupled to construct computational tools for rapid and accurate analysis of objects exposed to large fires. Application of the techniques to shipping containers for hazardous materials will allow more accurate simulation of both regulatory and accident fire conditions.

* This work was sponsored by the United States Department of Energy under Contract DE-AC04-94AL85000.

## DISCLAIMER

Portions of this document may be illegible in electronic image products. Images are produced from the best available original document.

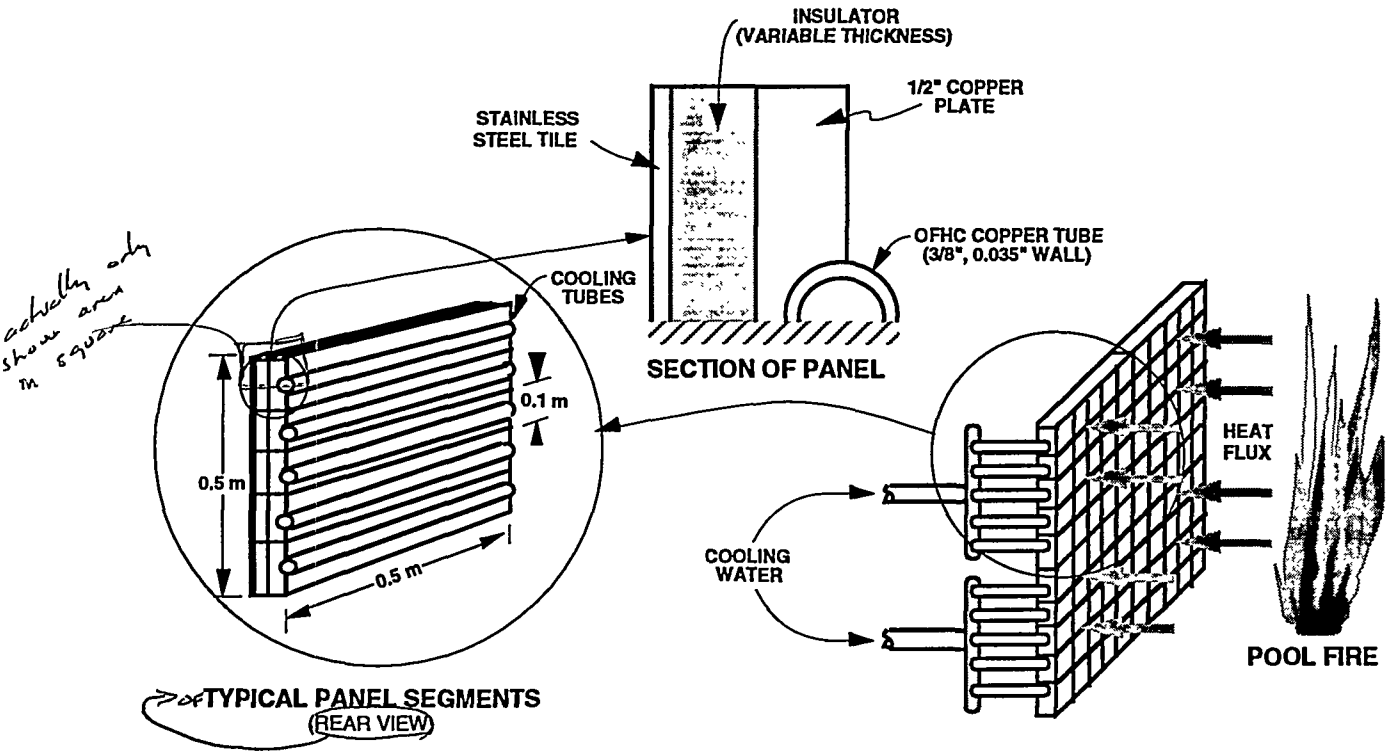


Figure 1. Sketch of actively cooled calorimeter.

The experimental measurements were conducted at the Sandia burn site in Coyote Canyon near Albuquerque, NM. The outdoor test was conducted in the 6 m x 6 m pool in conjunction with testing of an actual shipping container. The indoor tests were conducted at the SMokE Reduction Facility (SMERF), a facility designed to permit indoor testing of shipping containers [7]. SMERF is a new wind shielded indoor fire testing facility at Sandia National Laboratories intended for the thermal qualification of radioactive material packages that must meet Title 10, Code of Federal Regulations, Part 71 (10CFR71) and similar regulations such as the International Atomic Energy Agency Safety Series 6. SMERF has a 3 m x 3 m x 0.6 m pool for JP-4 fueled fires centered in the floor of a test chamber that is 6 m on a side and 14 m high. The walls of the chamber are water cooled to provide an appropriate boundary condition for radiative heat loss from the flames; this provides part of the control of the temperature in the flames. Air flow into the chamber is controlled by four variable speed fans with a nominal maximum capacity of 12000 scfm each. The facility includes a passive after burner that minimizes the smoke plume produced from the fire in order to meet local air quality requirements. One purpose of the indoor tests reported here was to assess how closely the indoor fire environment simulated the outdoor pool fire environment.

## DESCRIPTION OF CALORIMETER

The calorimeter shown in Figure 1 includes a 1 m x 1 m actively cooled surface. The cooled surface consists of 20 0.1 x 0.5 m copper plates with brazed 3/8 inch nominal diameter copper coolant tubes. Plates and tubes are arranged into 10 vertical zones. The copper plates are mounted with long stainless steel studs to a steel box frame that is enclosed with sheet metal and insulation. The long studs thermally isolate the copper plates from the steel frame. Stainless steel tiles (0.1 m x 0.1 m x 1.8 mm) form the surface that faces the fire. To provide high, uniform surface emittance, the tiles are coated with Pyromark Black. Calorimeter surface temperatures are controlled on an experiment-to-experiment basis by changing the thickness of the insulators located between the stainless steel tiles and the cooled copper plate. The stainless steel surface tiles are bolted with Belleville type spring washers to preserve good thermal contact even when heating causes differences in thermal expansion between the tiles and the insulating substrate.

For the outdoor experiment, 6.4 mm thick Macor ceramic insulators were used. Analyses show [8] that the calorimeter with these tiles should reach steady state in two to three minutes. For the indoor SMERF experiments, a 3.2 mm thick stainless steel feltmetal material, Technetics FR1109, was used as the insulator. Both insulators provide roughly equivalent thermal resistance to the surface. Water flow is distributed into upper and lower banks of five tubes as shown in Figure 1. The flow velocity in each tube is typically set for 2 m/s, resulting in water temperature rises of about 20 to 30°C. Water temperatures are measured with type K thermocouples. One inlet thermocouple is provided in each inlet manifold, while each of the ten tubes exiting the calorimeter has a separate thermocouple. To insure measurement consistency, all thermocouples were specified to be produced from the same batch of thermocouple wires. Water flow is measured in the upper and lower tube banks of five tubes each with two turbine type flow meters. To create an even flow distribution among the five tubes in each bank,

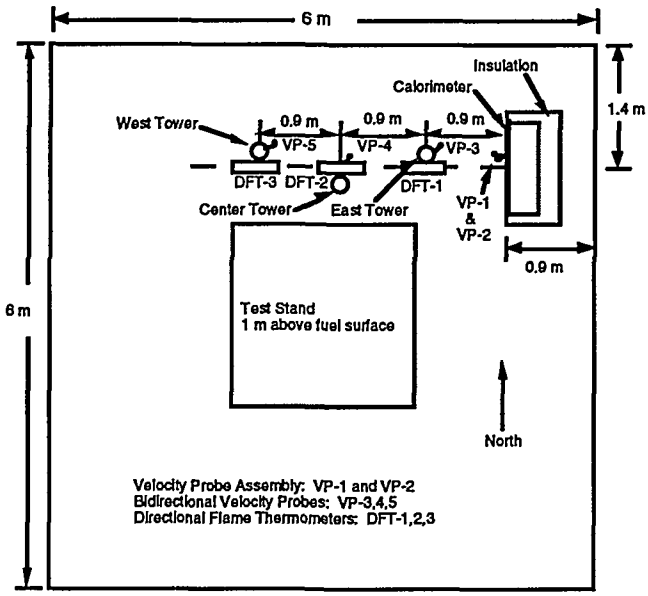


Figure 2. Sketch of open pool fire arangement as viewed from above pool.

pace

large diameter inlet and outlet manifolds are used to assure uniform tube entrance and exit pressures, and care was taken during assembly to assure that all copper tubes have the same shape and routing between the manifolds. Further details of the analysis leading to the design are provided in Reference [8].

Before performing any fire measurements, the calorimeter was tested in the Sandia radiant heat facility where banks of halogen-filled quartz lamps behind a steel shroud simulated the fire environment. Absorbed heat fluxes of 70 to 80 kW/m$^2$ were recorded. Under these conditions, the maximum recorded variation of a measured heat flux data point from a cubic polynomial fit through all ten data points was 2.7 %, with a rms variation of 0.5 % for the ten channels. The variations are most likely caused by small tube-to-tube differences in the water flow. The radiant heat testing also served to cure the Pyromark Black surface on the surface of the tiles.

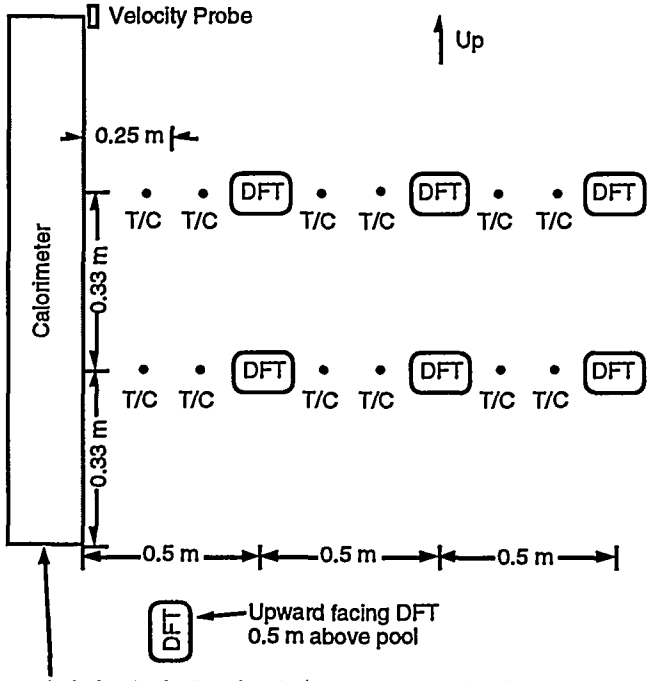


Figure 3. Fire diagnostic arrangement for SMERF tests as viewed from side of pool.

For the outdoor test, the calorimeter was mounted facing west near the northeast corner of the 6 m x 6 m pool as shown in Figure 2. The vertical plane of the face was 0.9 m west of, and parallel to, the east edge of the pool. The center of the vertical face was located 1.3 m above the pool initial fuel level and 1.4 m from the northeast corner. The location was chosen to minimize interference with a test object at the center of the pool. For the SMERF test, the calorimeter was located 2 m from the side the 3 m x 3 m pool, with the bottom edge approximately 1 m above the pool surface (see Figure 3).

Additional diagnostics included in the calorimeter structure itself are intrinsic thermocouples, radiometers, and various thermocouples for checking internal temperatures. The intrinsic thermocouples are formed by spot welding closely spaced type K thermocouple wires to the back of 18 of the stainless steel surface tiles. Locations of the intrinsic thermocouples are shown in Figure 4. During radiant heat testing the intrinsic thermocouples performed well with zones of higher temperature consistently coinciding with zones of higher heat flux. Four Schmidt-Boelter type radiometers with an 11° field of view are mounted (see Figure 4) behind holes in the copper plates and tiles. These radiometers have a much faster response than the water calorimetry, and are intended to provide a measure of the time variations of surface heat flux. Space limitations do not permit reporting the radiometer

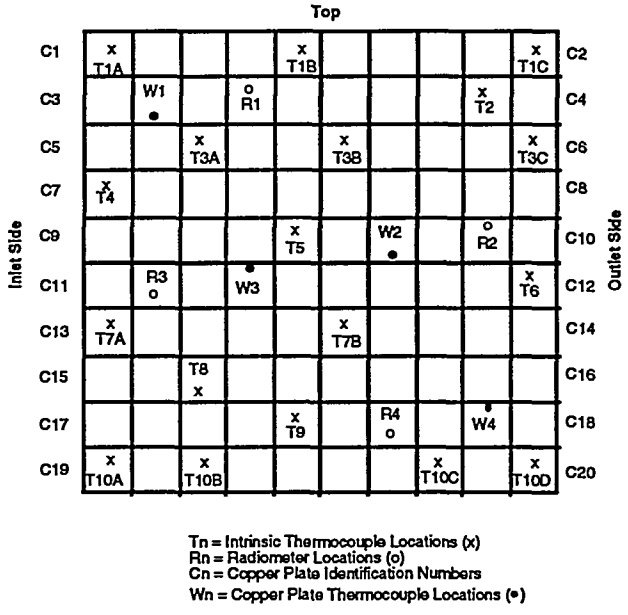


Figure 4. Location of diagnostics on front face of calorimeter. Small squares represent stainless steel tiles that face fire.

inconsistent tabbing?

results in this paper. Type K thermocouples monitor copper plate temperatures at the locations shown on Figure 4.

General fire diagnostics included a meteorological tower with wind velocity and direction measurements at various heights above the pool, and video records of the fire from three directions.

## OTHER FIRE DIAGNOSTICS

### Directional Flame Thermometers

Directional flame thermometers (DFTs) were included as part of the fire instrumentation package. A DFT consists of a plate that is insulated on the back side, and exposed to the fire on the other side. A type K thermocouple is mounted on the back face.

The plate is a thin sheet of metal that rapidly reaches a thermal equilibrium with the heat flux incident on the front face. By assuming convection heat transfer is a small portion of the incident heat flux on the DFT surface, Fry [8] demonstrates that the temperature measured by the DFT approximates the black body temperature for the incident radiation, and hence the incident flux, on the DFT.

The outdoor test configuration consisted of three DFTs in an east-west line located 1.4 m from the northern edge of the fire fuel pool as shown in Figure 2. The DFTs were spaced 0.9 m apart and were located 1.3 m above the fire fuel pool. DFT 1 was the easternmost sensor and was 0.9 m from the front face of the calorimeter. DFT 3 was the westernmost sensor and DFT 2 was located between DFT 1 and 3. Each DFT had an eastern and a western facing sensor plate. For the indoor tests, two horizontal rows of three DFTs each were used with sensors facing toward and away from the calorimeter face as shown in Figures 3.

In addition the the DFTs, 1.6 mm diameter, inconel sheath, ungrounded junction, type K thermocouples were supported in the flame region. For the outdoor tests, the thermocouples were located with tips facing upward in between the DFTs, at distances of 1.4 and 2.3 m from the calorimeter front surface. The height above the pool for the thermocouples is the same as for the DFTs, 1.3 m. For the indoor tests two thermocouples were located between DFTs as shown in Figure 3.

### Velocity Probes

There are several problems in measuring the gas velocity in the fire plume of an open pool fire. The fire plume is very turbulent with large fluctuations caused by air entrainment, mixing, combustion processes, and wind perturbations. Typically the gas velocities are low, the gas density is low and the temperatures are high. To avoid these problems a bi-directional, low-velocity pitot type probe designed for use at low Reynolds numbers was selected. Bi-directional probes have been used to measure velocities in large open pool fires because they are relatively insensitive to changes in flow direction [9].

To interpret the results from the vertical plate calorimeter, it is necessary to understand the flow velocity and direction across the face. The design and application of these "multi-directional probe assemblies" are described in detail in [10].

The velocity probe assembly was mounted above the center of the actively cooled surface as shown in Figures 2 and 3. For the outdoor test, a bi-directional velocity probe was installed at each DFT location to measure the vertical gas flow component. For the SMERF tests, a 3 m high tower with three bi-directional velocity probes was located halfway between the DFT array and the side of the pool to the right when facing the calorimeter face. To prevent deterioration, all the probes were coated with sol-gel/glass powder film [11] and the pressure sensing lines were water cooled and insulated with several layers of blanket insulation.

A 1.6 mm O.D., Inconel sheathed, ungrounded junction, type K thermocouple was used at each probe location to measure the temperature of the gas. These temperatures were used to calculate the density of the gas (assumed to be air) which in turn was used to calculate the gas velocity. Assuming that the gas is air could lead to errors in the lower flame region where it is expected that significant fractions of unburned fuel vapors may be present.

## OUTDOOR RESULTS

### Outdoor Calorimeter Surface Heat Flux

Heat fluxes calculated by water calorimetry for five zones ranging from 0.8 to 1.3 m above the fire for times from 10 minutes to 25 minutes after ignition are shown in Figure 5. The heat fluxes shown represent the absorbed energy to the water and were calculated from the equation

$$q'' = \rho V A_{tube}(h_{out} - h_{in}) / A_{plate} \qquad (1)$$

where q" is the heat flux to the zone in $kW/m^2$, $\rho$ is the inlet water density in $kg/m^3$, V is the inlet water velocity in a tube in m/s, $A_{tube}$ is the cross section area of a tube in $m^2$, $h_{out}$ is the outlet enthalpy in J/kg, $h_{in}$ is the inlet enthalpy in J/kg, and $A_{plate}$ is the surface area of the copper plate facing the flames. Water enthalpies were evaluated from a polynomial fit to steam table data for subcooled water at 0.2 MPa, close to the actual pressures in the tubes.

Two trends are visible in the data shown in Figure 5. First, with the exception of a period near 20 minutes after ignition, the heat flux generally decreases with height above the pool, and, second, the heat flux levels decrease with time. The observed decrease of heat fluxes with time, when correlated with several other measurements, is thought to be related to a decrease in wind speed that was observed during the fire. Further discussion of wind speed during the test is presented later. The small channel-to-channel scatter in heat flux at various heights indicated in Figure 5 are probably caused by flow variations between the coolant tubes, and are not considered to be significant.

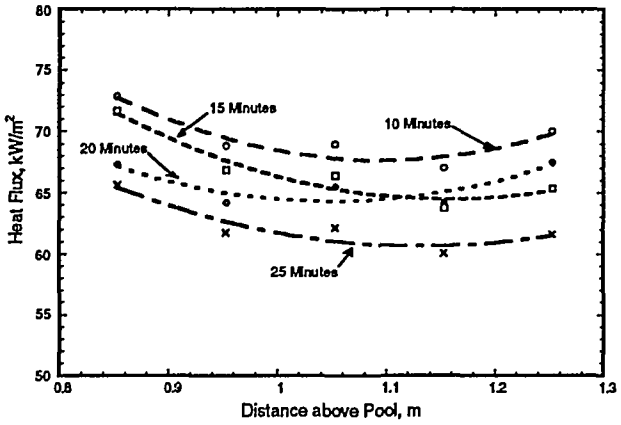


Figure 5. Abosrbed calorimeter heat flux at four times vs. distance above pool surface.

The heat flux data shown in Figure 5 represent only five of the ten channels available. The data from upper five channels representing heights of 1.3 to 1.8 m above the pool were discarded after examination revealed two problems. First, a flow blockage due to a metal chip caused abnormally high temperature rises in the zone just above the center of the calorimeter surface. Since this tube was manifolded with the four tubes above it, this cast doubt on the accuracy of all these data. Second, video observations showed that the upper half of the calorimeter, particularly the upper corner nearest the corner of the pool, was frequently not in contact with the flames during the fire. Data traces from the upper channels showed much wider variations of heat flux with time than the lower channels.

## Outdoor Calorimeter Surface Temperature

As shown in Figure 6, calorimeter surface temperatures, as estimated from the intrinsic thermocouples, ranged from 350°C to 650°C. The temperatures, in a manner consistent with the heat flux record, showed a gradual decrease with time during the test. The central area of the calorimeter typically exhibited the highest temperatures with the upper left and lower right corners (as viewed from the front) exhibiting lower temperatures.

The plots in Figure 6 were prepared by fitting a polynomial expression in the least squares sense to the data from 17 of the intrinsic thermocouple locations shown in Figure 4. The polynomial expression used was

$$T_1 = b_{00} + b_{10}\,x + b_{20}\,x^2$$

$$T_2 = b_{01}\,y + b_{02}\,y^2 \qquad (2)$$

$$T_3 = b_{11}\,xy + b_{12}\,xy^2 + b_{21}\,x^2y + b_{22}\,x^2y^2$$

$$T = T_1 + T_2 + T_3$$

where T is the temperature estimate, the $b_{nm}$ are the fit constants, and x and y are the horizontal and vertical distances from the lower left corner of the calorimeter as viewed from the front. With this technique, the maximum residual (i.e., the difference between fit value and measured value) for the outdoor test was typically 70°C, with most residuals ranging from 10 to 20°C. The data from thermocouple T2 in Figure 4 was discarded because it consistently read about 100°C higher than surrounding thermocouples, indicating a high contact resistance between the stainless steel tile and the ceramic substrate.

## Outdoor Calorimeter Surface Velocity Probe

The velocity history across the face of the calorimeter is shown in Figure 7. The flow velocity typically varies between 2 and 6 m/s. The flow direction varied in a sinusoidal fashion at angles in the plane parallel from the face of the calorimeter

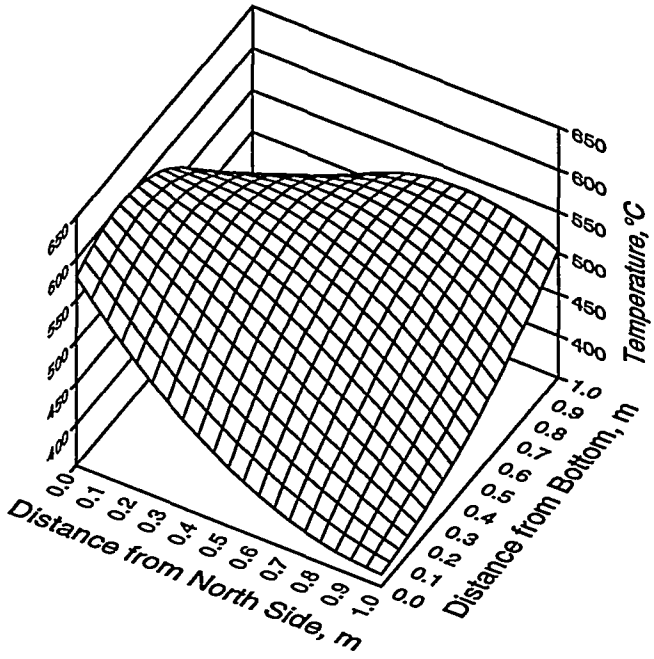


Figure 6. Surface temperatures at 15 minutes after ignition as estimated from intrinsic thermocouples.

ranging from 100 to 200°, where upward vertical flow corresponds to 180°. This variation is probably due to changes in wind direction.

## Outdoor Fire Environment Velocities

The velocity histories for the three towers are shown in Figure 8. These velocities agree in general with the velocity across the face of the calorimeter, especially for the East tower which is closest to the calorimeter. Within the region of time between approximately 6 and 11 minutes, the gas velocities within the fire, as given in Figure 8, exhibit no consistent trends, so quasi-steady state conditions were assumed. In particular, the West tower velocity fluctuates in a uniform fashion about a mean of approximately 6 m/s during this time period.

## Outdoor Emissive Power and Flux Distribution

The emissive power distribution, as measured by the two sheathed thermocouples suspended in the flame region and time-averaged over 350-710 s (5.8 to 11.8 min), is shown in Figure 9. Note that, to determine the average emissive power, the average of the fourth order temperature is required and not the average temperature to the fourth power. As shown in Figure 9, a polynomial curve fit to data derived from the two thermocouples of the average fourth order temperature distribution is almost linear. The third point at the left end of the curve represents data derived from an intrinsic thermocouple at the calorimeter surface.

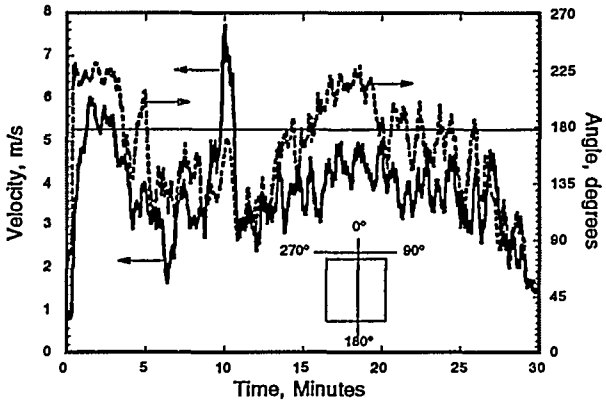


Figure 7. Velocity and flow angle in the plane parallel to the face of the calorimeter. Note that angle shows direction of source of flow, i.e., 180° represents vertical upward flow.

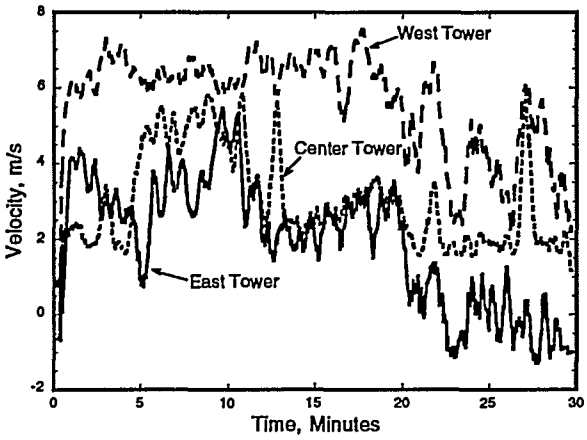


Figure 8. Velocities from bi-directional probes on towers in pool.

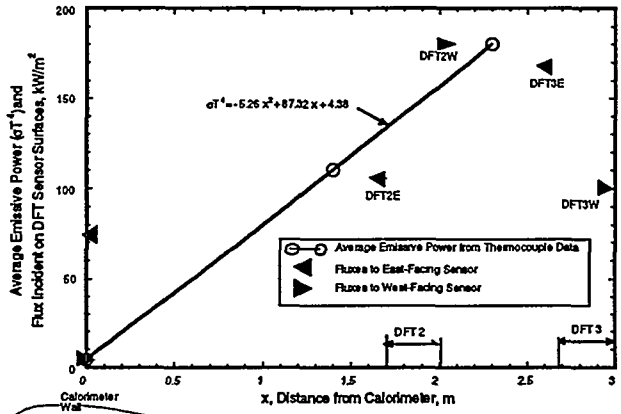


Figure 9. Emissive power estimated from thermocouples and Directional Flame Thermometers.

Heat fluxes derived from DFT temperatures (the results from DFT 1 followed a consistent trend but were omitted from the analysis due to its proximity to the calorimeter) are also shown in Figure 9. Assuming that the DFTs are in equilibrium (i.e. any energy storage in the instrument is negligible compared to the incident fluxes), and the DFT surfaces are gray and diffuse, then the heat flux incident on the instrument surface is equal to the flux being emitted and is given by $\sigma T^4_{DFT}$. Assuming the wall reflectively to be negligible, the flux incident on the calorimeter wall, i.e. the flux to a west-facing sensor at $x = 0$, is given by the sum of the absorbed heat flux, as determined by water calorimetry, and the emissive power given by the calorimeter surface temperature.

The flux distribution, as measured by the DFTs, is consistent with the average temperature distribution measured with the sheathed thermocouples located between the DFTs. The flux to all sensors facing east (towards the calorimeter) is lower than the local emissive power. This trend is expected for media with a finite optical path length since the sensor is "viewing" a temperature distribution which is, for the most part, at a temperature less than the local temperature. In general, and in keeping with the same trend, the fluxes to west-facing sensors are larger than the local emissive power since they are exposed to a higher temperature distribution due to the presence of the majority of the plume. An exception is observed at $x = 3.0$ m. The flux to a west-facing sensor at this point, DFT3W, is lower than the local emissive power. The lower flux measured at DFT3W tends to indicate a lower emissive power distribution to the right of the sensor rather than the increasing emissive power distribution given by the curve fit. Further investigation of the flux distribution shows that the flux at DFT3E is less than the flux measured at DFT2W. This observation is consistent with the emissive power distribution reaching a maximum near the pool centerline between $x = 2.0$ m and $x = 2.6$ m.

## Outdoor Effective Absorption Coefficient Estimation

Radiative heat transport is the dominant mode of energy transfer in these large pool fires. In order to model the interaction between the fire environment and the surface of an object, the radiative properties must be quantified. Knowledge

of the emissive power and heat flux distributions allow effective gray gas properties which are calibrated for two-flux radiative transport methods to be determined. These effective properties are required for analytical fire models which can function as part of an overall tool for the design and assessment of fire-survivable systems [6].

With the emissive power and flux distribution shown in Figure 10, an analysis of the effective absorption coefficient was performed by using a two-flux method to obtain an inverse problem solution to the radiative transfer equation within zones defined by the locations of the DFTs. The results are summarized in Table 1. Two independent solutions may be obtained by tracking fluxes in the negative and positive directions. The agreement between absorption coefficients calculated from balancing fluxes in the two directions is reasonably good (within 30%) for the zone closest to the calorimeter surface. The average of the two absorption coefficients is 0.83 $m^{-1}$. Therefore, the effective absorption coefficient within this region is slightly less than 1 $m^{-1}$. Inspection of the video record indicated, that, due to the intermittent flame cover, the absorption coefficient in this zone would be small. The value obtained from the analysis agrees well with the expected trend.

A considerably larger variation is observed for the zone farthest away from the calorimeter. This discrepancy can be attributed to the uncertainty inherent in the temperature distribution for 1.85 m < x < 2.38 m. As previously noted, the flux data indicates that the plume centerline is between 2.0 m and 2.64 m. Due to a lack of data, characterization of the temperature within this zone was not possible. However, both values of the effective absorption coefficient calculated for this zone are greater than 1 $m^{-1}$, indicating that the optical thickness increases towards the interior of the plume.

**Table 1: Effective Absorption Coefficient Calculation**

| Zone | From Balance of Fluxes in Negative Direction | From Balance of Fluxes in Positive Direction | Average |
|---|---|---|---|
| 0 <x< 1.85 m | 0.7 $m^{-1}$ | 0.95 $m^{-1}$ | 0.83 $m^{-1}$ |
| 1.85 m <x< 2.38 m | 3.1 $m^{-1}$ | 1.5 $m^{-1}$ | 2.3 $m^{-1}$ |

The effective absorption coefficients given in Table 1 were determined at an elevation of 1.3 m from the pool surface. A preliminary, proof of concept, analysis provided an estimate of 3.6 $m^{-1}$ for the effective absorption coefficient at an elevation of 1.2 m in the interior of a JP-4 plume located alongside a tractor-trailer wall. Therefore, a value between 1.5 $m^{-1}$ and 3.1 $m^{-1}$ appears to be reasonable. The above effective absorption coefficient values begin to illustrate the trends that can be used to form a library of model input parameters.

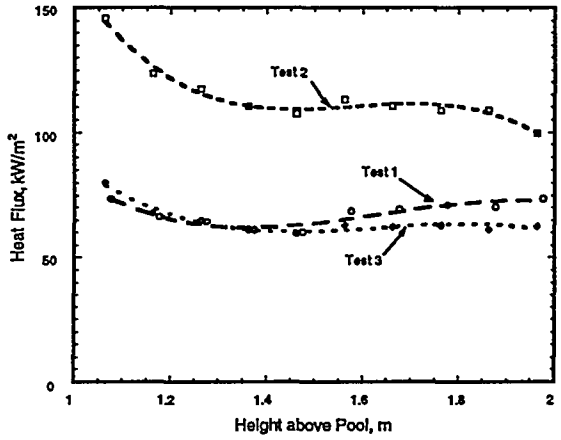


Figure 10. Absorbed heat fluxes nine minutes after ignition measured during three successive tests in SMERF.

## INDOOR RESULTS

### Indoor Calorimeter Surface Heat Fluxes

For the indoor tests, all calorimeter channels were operational giving heat flux variations over the full height of the calorimeter as shown in Figure 10. The time at 9 minutes after ignition was selected as typical of the data observed. In all tests, heat fluxes tended to have a peak near the bottom of the calorimeter. The test-to-test variation is attributed to configuration changes inside SMERF. For the second test, rolls of mesh used to reinforce concrete were stood at several locations along the inside wall of SMERF. The increased turbulence apparently increased the heat fluxes over the first test. For the third test the rolls of reinforcing materials were removed to the same configuration as the first test, and the fan speed lowered from 11.3 standard $m^3/s$ (24,000 scfm) on the first two tests to 10.4 standard $m^3/s$ (22,000 scfm).

### Indoor Calorimeter Surface Temperatures

Calorimeter surface temperatures during the indoor tests were much more uniform than those observed during the outdoor test. Figure 11 shows the results for the third test in the series. The polynomial fit to intrinsic thermocouple values for the indoor tests was also much better than for the outdoor tests with maximum residuals in the 10°C range.

### Indoor Calorimeter Surface Velocity Probe

Velocities and directions for the directional probe assembly for the third test are shown in Figure 12. The velocities are roughly comparable to the outdoor test, but the directions are more variable with predominant upward and left to right directional swings. Tower velocities for the third test are shown in Figure 13. Velocities at all three heights are comparable at about 5 m/s.

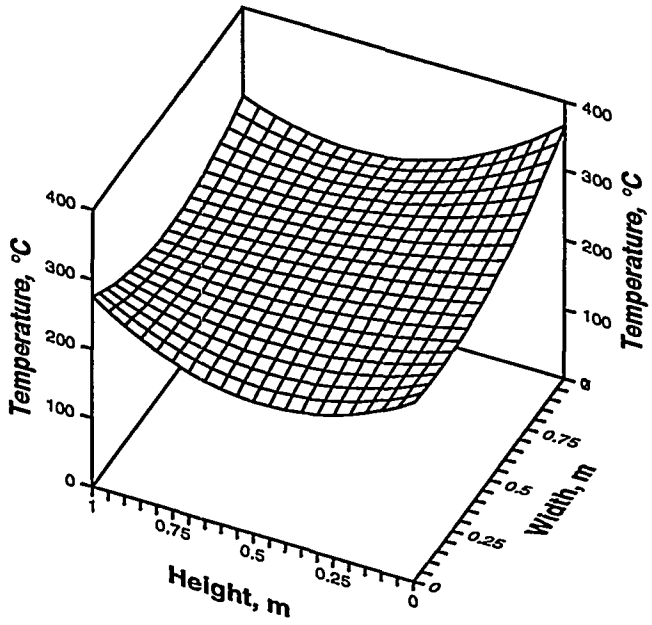


Figure 11. Calorimeter surface temperatures at nine minutes after ignition for third indoor test.

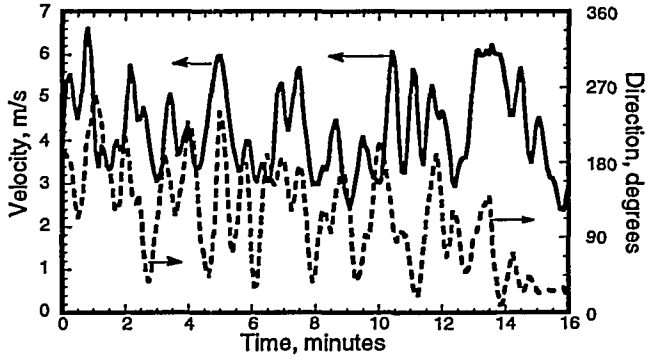


Figure 12. Velocities and directions across calorimeter face for third indoor test.

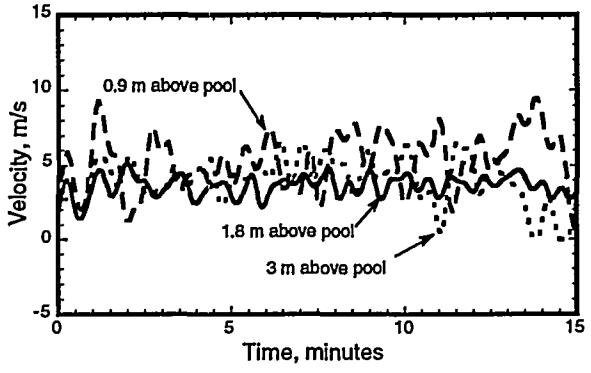


Figure 13. Tower velocities for third indoor fire test.

## Indoor Temperature Distribution

The time-temperature distribution for a typical indoor test, as measured by the sheathed thermocouples is shown in Figure 14. The temperature range is between 800°C and 1000°C, and is similar to what has been measured for large outdoor pool fires.

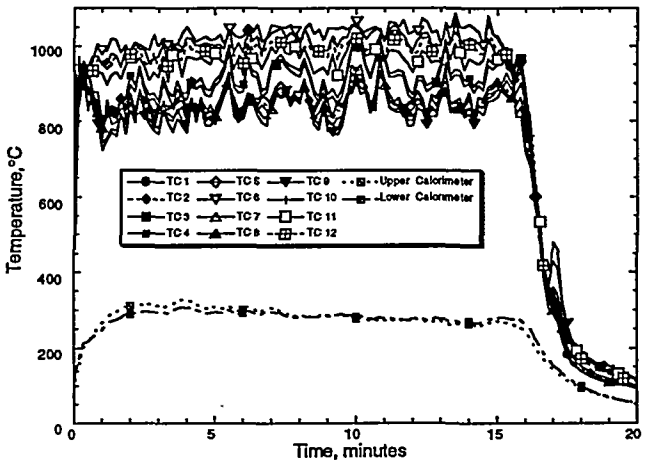


Figure 14. Flame temperature data for first indoor fire test. Direction of flow is defined consistently with Figure 7.

## Indoor Emissive Power and Flux Distribution

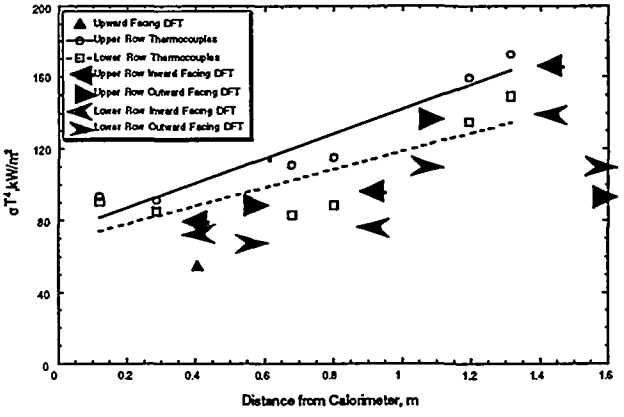


Figure 15. Time averaged emissive power and flux distribution for first indoor fire test.

The flux distribution, as measured by the DFTs, is shown in Figure 15. The DFT values are lower than the emissive power measured with the sheathed thermocouples located between the DFTs. This trend is expected for media with a finite optical path length since the sensor is "viewing" a temperature distribution which includes temperatures less than the local temperature. The heat fluxes and emissive power increase with increasing distance from the calorimeter. The DFTs furthest

from the calorimeter are close to the edge of the pool and face outward. It is expected that the fluxes incident on this gauge are a result of emission from a temperature distribution that extends past the fire boundary. The heat fluxes measured with the DFTs are between 70 and 160 $kW/m^2$, the magnitude of which are comparable to the heat fluxes measured in an open outdoor pool fire.

The emissive power and heat flux distribution in the vertical direction shows a consistent rise in emissive power and heat flux from the lower to the upper row of instrumentation. This trend has also been observed in large outdoor pool fires.

An estimate of the effective absorption coefficient was performed with the same technique as described for outdoor tests. The result of the analysis for the zone between the calorimeter front face and the first DFT station, a distance of 0.5 m, produced an absorption coefficient estimate of between 2 and 3 $m^{-1}$, which is comparable to absorption coefficients calculated for outdoor pool fires. Larger variations in the heat flux balance used to calculate the absorption coefficient occured for the zones further away from the calorimeter front face. The variations are potentially due to a variety of causes related to use of the indoor facility. For example, the forced input of combustion air from the fans is significantly different from the free boundary air entrainment of outdoor fires. This difference could lead to such effects as hot and cold zones in the indoor fire depending on local fuel-air mixtures and flow velocities. For outdoor fires, radiation is typically the dominant heat transfer mechnanism. This has yet to be proven for the indoor test facility where fans may contribute to a stronger convection mechanism.

## CONCLUSIONS

The use of an actively cooled calorimeter provides a different perspective on long-term fire trends than an uncooled calorimeter based on transient analysis. As long as the actively cooled surface maintains a nearly constant temperature, trends can be observed without the necessity of first unraveling the interdependence between heat flux and surface temperature.

The general trend toward a decrease in measured heat flux with increased height above the pool shown in Figures 5 and 10 is consistent with the gray gas model developed by Nicolette and Larson [3] for a constant temperature vertical flat plate. In that model, soot is modeled as a gray gas that participates in the radiant heat transfer between the core of the fire and a constant temperature plate. As soot-laden gas moves up the front face of the vertical plate, the presence of the cold plate convectively and radiatively cools the soot. As the soot cools, it absorbs and emits radiation at lower temperatures, and, as a result, heat flux to the wall decreases. While the initial testing is promising in confirming this effect, further tests will be necessary to ensure that the effect can be consistently measured and quantified.

For the outdoor test, one trend observable in many diagnostics is a general decrease in fire intensity as the burn progressed. These decreases may be related to a decrease in wind velocity that led to less fuel mixing later in the test. Decreases in both heat flux and surface temperatures of the calorimeter are observed, as well as decreases in temperatures measured by the DFTs. This is the type of effect that could be difficult to confirm with uncooled calorimeters, but is easily discerned with active cooling.

Shortly after 10 minutes into the outdoor fire test, highly transient responses are visible on several diagnostic traces (see Figures 7 and 8). Heat flux and surface temperatures temporarily increased, as did temperatures measured by some DFTs. Flow velocities in the pool, as measured by the velocity probes at the East and Center towers, dropped at the same time. Radiometer data not presented also indicated a significant drop in heat flux in this time frame. Inspection of the video record shows that flames appeared over the top of the calorimeter at this time in a region that was generally clear during the burn. No large changes in wind direction or velocity were observed during this period, so the cause of this behavior is uncertain.

For the outdoor test, temperature distributions on the front face of the calorimeter also raise some questions. Both the upper left and lower right corners, as viewed from the front, exhibited lower temperatures than the rest of the face. This pattern was confirmed by differences in appearance of the stainless steel surface tiles observed after the test. The cooler corners appeared sooty and black, while the hotter regions appeared more reflective and metallic. The soot pattern in the tiles also indicated a general upward and to the right skew of the flow velocities across the face. The effect on the upper left corner can be explained by the fact that this portion of the calorimeter was in and out of the flame region during the test, but the cause of the effect at the lower right corner is more difficult to determine. One possible cause is a steel channel support that extended from the bottom of the calorimeter support table and sloped slightly outward toward the pool center. For the indoor tests much more uniform surface temperatures were observed.

The lack of success in applying the outdoor fire model to the indoor fire environment indicates a fundamental difference in the fires although the flame temperatures and heat fluxes are quite similar. Estimates of absorption coefficients from the fires are in the 1 to 3 m range. This is consistent with values given in the literature for large pool fires. For modeling of containers to be tested in the SMERF facility, a simple empirical model of heat flux vs. height above the pool may prove to be more useful than attempting a detailed model with participating medium effects.

Further tests with the calorimeter will aim at continuing to develop the experimental data base of fire measurements that will be useful in constructing a simple large pool fire model for use in the design and analysis of shipping containers for hazardous materials. An extended outdoor series is planned to study such effects as height above the pool, surface orientation, and surface temperature. Use of the measurements will allow computer models to be fast and simple enough to be used as a subroutine to finite element thermal codes.

## REFERENCES

1. Gregory, J. J., Keltner, N. R. , and Mata, R., Jr., "Thermal Measurements in Large Pool Fires, Journal of Heat Transfer, " No. 111, pp. 446-454, 1989.

2. Gregory, J. J., R. Mata, Jr., and N. R. Keltner, "Thermal Measurements in a Series of Large Pool Fires," SAND 85-0196, Sandia National Laboratories, Albuquerque, NM, 1987.

3. Nicolette, V. F., and Larson, D. W., "The Influence of Large, Cold Objects on Engulfing Fire Environments," Proceedings of AIAA/ASME Thermophysics and Heat Transfer Conference, Seattle, WA, June 18-20, 1990.

4. Burgess, M. H., and Fry, C. J., "Fire Testing for Package Approval," Radioactive Material Transportation, Vol. 1, No. 1, pp. 7-16, 1990.

5. Gritzo, L. A. and Nicolette, V. F. "Coupled Object Response of Objects and Participating Media in Fires and Large Combustion Systems," Heat Transfer in Fires and Combustion Systems, ASME HTD-Vol. 250, pp. 161-169, 1993.

6. Gritzo, L. A.; Moya, J. L. and Nicolette, V. F., 1993, "Use of Simplified Deterministic Fire Models to Estimate Object Response for Probabilistic Fire Safety Assessments," Proc. of the NIST Annual Conference on Fire Research, Rockville, MD, October 18-22, 1993.

7. Keltner, N. R. and Kent, L. A., "A Wind Shielded Fire Test Facility," in Proc. of The 9th Symposium on the Packaging and Transportation of Radioactive Materials, July 11-16, 1989, Washington, D.C., CONF-890631, prepared by Oak Ridge National Laboratory, 1989.

8. Koski, J. A., Keltner, N. R., and Nicolette, V. F. , "Design of an Actively Cooled Plate Calorimeter for the Investigation of Pool Fire Heat Fluxes", in Proc. 10th Symp. on the Packaging and Transportation of Radioactive Materials, Yokohama, Japan, September, 1992.

9. Kent, L.A., and Schneider, M.E., "The Design and Application of Bi-directional Velocity Probes for Measurements in Large Pool Fires," ISA Transactions, 26, #4, pp. 25-32, 1987. (also as ISA Paper # 87-0203).

10. Newman, J.S., "Mult-Directional Flow Probe Assembly for Fire Application" Journal of Fire Sciences, Vol 5, No. 1, 50-56, (January/February 1987).

11. Brinker, C.J., Reed, S.T., "Low Temperature Process for Obtaining Thin Glass Films" (Patent Number 4476156, October 1984), Sandia National Laboratories, Albuquerque, New Mexico.